THERMAL DEGRADATION ASSESSMENT OF KRAFT PAPER IN POWER TRANSFORMERS INSULATED WITH NATURAL ESTERS

Inmaculada Fernández[1], Fernando Delgado[1], Félix Ortiz[1], Alfredo Ortiz[1], Cristina Fernández[1], Carlos J. Renedo[1], Agustín Santisteban[1]

University of Cantabria
Avenida de Los Castros
39005, Santander. Cantabria (Spain)
Electrical and Energy Engineering Department
E.T.S. de Ingenieros Industriales y de Telecomunicación
(*) Corresponding Author Contact Details:
Tel: +34 942 201 374 – +34 626 966 431
Fax: +34 942 201 385
ortizfa@unican.es

1. Introduction

Electricity distribution and transmission require the use of power transformers, so they are vital and strategic components of any electric power system [1-4]. It is known that the failure of power transformers can produce significant economic losses related to its reparation or replacement as well as financial losses compensations required by consumers [4-5].

The life span of transformers is basically determined by physicochemical, electrical and mechanical characteristics of their insulation system [6, 7]. This insulation system generally consists of two types of materials, liquid and solid [8]. In power transformers, solid insulation is frequently based on cellulose which is used in different forms (paper, press-board...). The most common is Kraft paper, a mix of 78-80% cellulose, 10-20% hemicellulose and 2-6% lignin [9]. This paper is the main solid insulator for the winding conductors. As insulator, the dielectric paper is a material that avoids the flow of electric current among conductors. Solid insulation is impregnated with dielectric oil which is also used as cooling medium [10]. In the case of a 150 MVA transformer it may contain as much as 80 tons of oil and up to 30 tons of paper. This insulation system under operational conditions suffers electrical, thermal, environmental and mechanical stress due to the presence of traces of air and water which worsen electrical properties of paper and oil [5, 11]. Although, oil can be easily reclaimed or substituted this will not extend the cellulose's life [2]. For this reason, the degradation of cellulose-based paper determines the useful life of a power transformer [12]. Cellulose degrades slowly but inevitably losing its mechanical properties [13] due to the breakage of glycosidic inter-monomer bonds in the polymer which reduces the chain-length [14]. Failure occurs when the mechanical strength of the paper decreases to the point where it is brittle and liable to damage by mechanical movement. This might result from load changes, or from the flow of oil over the paper, although other factors can cause failure to occur early [15]. Thus, accurate information regarding the degradation process of solid insulation can be determined through the evolution of the degree of polymerization (DP) with time [16, 17]. The DP of cellulose is a standard method of quantifying cellulose degradation, so that, the lower the DP of a sample, the greater the degradation. The DP value indicates the average polymer length of the cellulose molecules. This method is effective for quantitative measure of thermal aging [18].

On the other hand, the most commonly used oil in power transformers is mineral oil because of its cost and physical and dielectric properties [4]. This kind of dielectric oil has low flash and fire points. However, the most serious of its shortcomings is the inability to meet new health and environmental regulations because it is not biodegradable. Additionally, the naphthenic crude oil reserves from which mineral oil is obtained are limited. These disadvantages led the search for new fluids. Different dielectric oils (silicone oils, high molecular weight hydrocarbons, synthetic and natural esters) have successively been made available in the market [4, 19]. Natural esters, having the advantages of high biodegradability, fire safety and abundant supply, might be the most ideal substitute for mineral oil [4]. When a new material is to be introduced to a system, the rate of degradation of the insulation in the presence of different kind of stress should be evaluated in order to be able to use it with confidence [20].

So far, there has been a lot of research about cooling improvement in power transformers using mineral oil [21-24]. The reason is that hottest spot temperature inside windings of the oilimmersed power transformers is one of the main manifestations of the thermal stress which leads to aging and decomposition of both liquid and solid insulation material (oil and cellulose) more rapidly as compared with less heated spots [25-27]. Although some studies have examined the aging of dielectric paper submerged in mineral and vegetable oil [6, 28], all of them have taken into account that both liquids have the same cooling capacity. In this work it has been considered that the temperature at which paper is subjected depends on the type of oil used in the transformer.

This work has used a 3D-section of the cooling ducts of the low voltage winding (LVW) of a real power transformer to analyze the thermal-fluid behavior of three dielectric liquids (two vegetable oils and a mineral one). For these fluids, the hot-spot temperatures are obtained in order to establish the severest condition suffered by the dielectric paper. Later, thermal differences have been applied in accelerated thermal aging experiments. The aim is to examine the influence of temperature on the degradation of Kraft insulating paper in transformer oil based on natural esters.

Regarding the organization of this paper, the second section of this work assesses the temperature and velocity distributions of mineral and vegetable oils in a transformer. In the third section, the method used to study the DP of the dielectric paper by means of aging tests is presented. The conclusions of this study which could expand current knowledge on Kraft paper aging in vegetable oil immersed transformers are explained in the fourth section

2. Thermal-hydraulic simulation of dielectric oils

In power transformers a quite small part of the electrical energy is converted to heat which causes significant temperature rise. This fact limits not only the transformer operation; it leads also the degradation of insulating system in power transformers. For this reason, it is critical to estimate the hottest spot temperature (HST) to avoid rapid thermal degradation of insulation systems and subsequent breakdown. In order to determine the temperature that the Kraft paper suffers in a power transformer refrigerated by insulating liquids, the thermal-hydraulic behavior of three dielectric oils has been simulated in specific transformer geometry. Two of these liquids are based on vegetable esters and the other one is a mineral oil. The software used is based on Finite Elements Method (Comsol Multiphysics).

2.1. Model geometry

A section of the Low Voltage Winding (LVW) of a three-phase power transformer has been used in order to carry out the simulations. In the High Voltage Winding (HVW) the electric current is lower. In fact, in this case, the copper losses at power rated of the HVW are 8% smaller that those of the LVW so that less heat is generated and the HST is less critical. The main characteristics of this transformer are: 14 MVA, 66/6.3 kV, Dyn11 and Oil Natural/Air Natural (ONAN) cooling. Transformers of this capacity -or similar- and with this type of cooling can be found frequently in the distribution networks worldwide.

The self-explanatory Fig. 1 shows the three windings of a phase of a three-phase transformer: LVW in the inner part; on-load tap winding in the outer part; finally, the High Voltage Winding in the middle of the other ones.

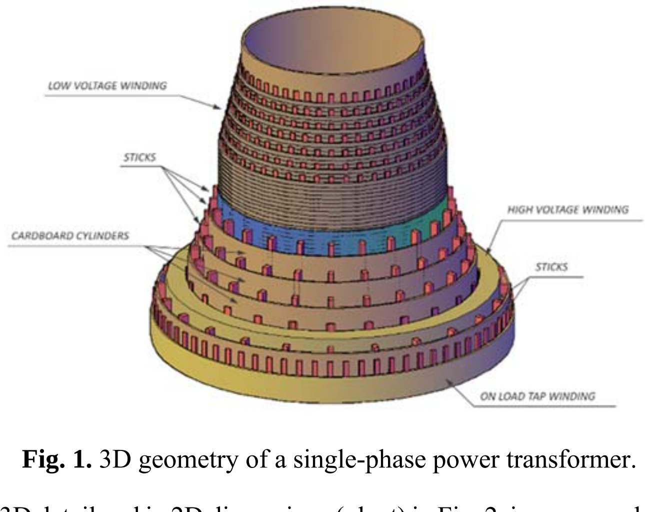

Fig. 1. 3D geometry of a single-phase power transformer.

The LVW, shown in a 3D detail and in 2D dimensions (plant) in Fig. 2, is composed of an internal cardboard cylinder (6 mm thick and 450 mm of inner diameter) surrounded by 7 concentric layers with 11 copper turns by layer. Each turn has 8 parallel plates (plate dimensions: 10.4 mm x 4.6 mm) that are wrapped with a dielectric paper of 0.3 mm width. The layers are separated by means of 48 wooden sticks and inter-sticks of 3 mm thick. This way, 48 cooling ducts of 7.5 degrees of amplitude are created between internal cylinder and first layer, other 48 cooling channels between first layer and second layer, and so on. Finally, the total height of the LVW is 1,056 mm.

The Fig. 3 illustrates how the geometrical design has evolved to achieve the optimal one from the numerical point of view. No differences are appreciated in the results of the tested 15 degree model and the 7.5 degree model because the first one is divided in two symmetric volumes by the cut plane.

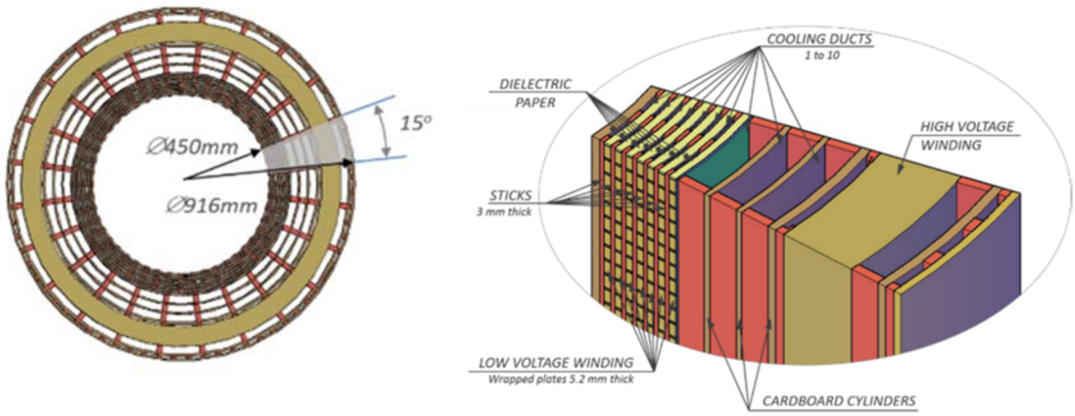

Fig. 2. Plant view of a phase and 3D detail

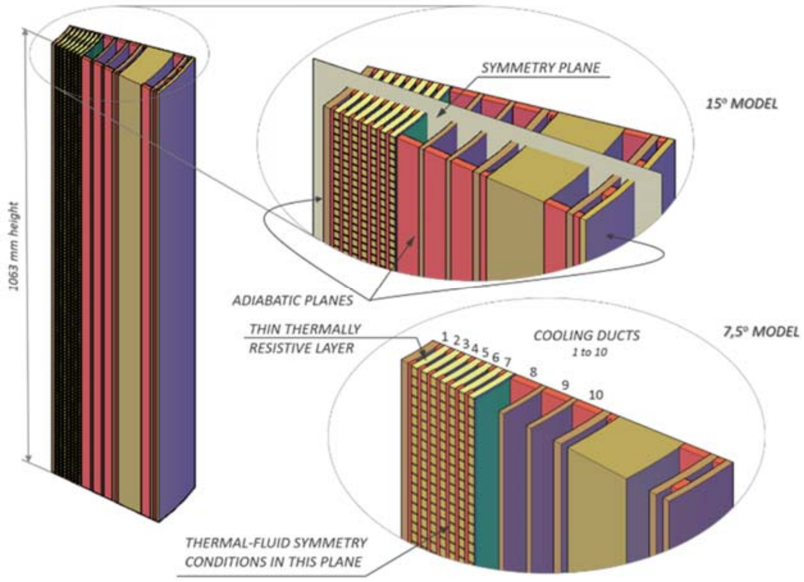

Fig. 3. Geometrical evolution of the model

2.2. Numerical model

This section present the numerical model applied on the 3D geometry explained in the previous subsection.

2.2.1. Governing equations

A steady state study is carried out using the Conjugate Heat Transfer model (CHT model) of the finite element-based software Comsol Multiphysics 5.0. This model combines the Fluid Dynamics (FD) and Heat Transfer (HT) physics. In the case of the FD physics, the main governing equations are the Navier-Stokes equations for incompressible fluids in stationary regime (See Eq. (1) and (2) in which the symbols ρ, $\mathbf{u}$, p, $\mathbf{I}$ and μ are density, velocity vector, pressure, identity matrix and dynamic viscosity, respectively. In eq. (2), $\mathbf{F}$ represents the buoyancy forces, while the other right-hand term represents the pressure and viscous forces, respectively).

$$\nabla \cdot (\rho \mathbf{u}) = 0 \quad (1)$$

$$\rho(\mathbf{u} \cdot \nabla)\mathbf{u} = \nabla \cdot \left(-p\mathbf{I} + \mu(\nabla\mathbf{u} + (\nabla\mathbf{u})^{\mathrm{T}}) - \frac{2}{3}\mu(\nabla \cdot \mathbf{u})\mathbf{I}\right) + \mathbf{F} \quad (2)$$

In relation to the HT physics, Eq. (3) is the energy equation that governs the heat exchange in the fluid and in the solid in steady state. In this equation, the symbols C_p, k and T are the specific heat capacity, thermal conductivity and temperature, respectively. Also, the term Q represents a heat source per volume produced by Joule losses in the copper of the LVW layers.

$$\rho C_p \mathbf{u} \cdot \nabla \mathrm{T} = \nabla \cdot (k\, \nabla T) + Q \quad (3)$$

2.2.2. Boundary conditions

The exterior walls of the model are considered to be adiabatic surfaces except for those located in the bottom. This assumption is based on several facts. For instance, the vertical radial walls are modelled as thermal-fluid symmetry planes. Regarding the inner and outer vertical walls, they can be considered as adiabatic surfaces since they are two cylinders that are made with cardboard, a very low thermal conductivity material. Finally, the heat exchange between horizontal upper solid surfaces and the coolant can be considered negligible based on the fact that the temperatures difference between both materials is very small (see Eq. (4) in which **n** is the normal vector to boundary surface).

$$-\mathbf{n} \cdot (-k\nabla T) = 0 \quad (4)$$

A convective heat flow between the bottom solid surfaces and the oil has been taken into account.

The oil inlet temperature, $T_{oil,inlet}$, in the cooling ducts has been set in 35ºC. This value is based on measures of the oil temperature when it leaves the radiator and goes into the transformer; this measurement was made with an infrared thermometer. The Eq. 5 is the boundary condition of convective heat transfer, where h is the convective heat transfer coefficient that is calculated considering the characteristic length L (area/perimeter).

$$-\boldsymbol{n} \cdot (-k\nabla T) = h \cdot (T - T_{oil,inlet}) \quad (5)$$

Most of the oil from the radiators entering the transformer tank will flow using the hydraulic circuit with low pressure loss. That is, it will flow between the outer part of the windings and the tank walls. Also, the surface of the tank bottom is much greater than those of the pipes outlets emptying the radiators. As a result of the above, the inlet velocity of the oil to the cooling ducts can be considered negligible ($u_{z=0} \approx 0$). So, natural convection due to the decreasing of the oil density with the temperature has been considered inside the cooling ducts. In fact, the buoyancy forces (**F**) resulted from this density differences are the only ones that are considered to produce the movement of the oil inside the cooling ducts (See Eq. (6) in which g is the gravity acceleration).

$$\mathbf{F} = -g \cdot \left(\rho(T) - \rho\left(T_{oil,inlet}\right)\right) \quad (6)$$

Also, pressure-based boundary conditions are fixed in inlets and in outlets of the cooling ducts (see Eq. (7) for inlet pressure and Eq. (8) for outlet pressure in which $T_{oil,\ avg}$ and H are the average temperature of the oil inside the ducts and the total height of the ducts, respectively).

$$p = \rho\left(T_{oil,\boldsymbol{avg}}\right) \cdot g \cdot H \quad (7)$$

$$p = 0 \quad (8)$$

A uniform volumetric heat source (Q) is considered in the copper conductors. This value is calculated using the Joule losses that are measured in a short-circuit test of the power transformer (see Eq. (9) in which P_{Joule} and V are the copper loses in the 3-phase LVW and the volume of this winding, respectively).

$$Q = \frac{P_{Joule}}{V} \tag{9}$$

No-slip condition is considered in the walls of the cooling ducts except for those which represent a symmetry plane (see Eq. (10)).

$$\mathbf{u} = 0 \tag{10}$$

All the wrapping paper is considered mathematically as a thin thermally resistive layer whose thermal behavior is modeled according Eq. (11) in which k_p, T_i, T_o and d_p are the thermal conductivity, the temperatures in the inside and outside surfaces and the thickness of the paper, respectively.

$$q = -k_p \frac{(T_i - T_o)}{d_p} \tag{11}$$

The type of cooling ducts (vertical channels), in addition to the high viscosities of oils, allows us to establish that the heat transfer is going to be carried out by natural convection under laminar flow regime. In order to confirm these assumptions, typical dimensionless parameters will be obtained in a subsequent section using simulation data.

2.2.3. Meshing and computational information

The whole mesh, shown in Fig. 4, consists in hexahedral elements. There are 1082880 domain elements, and also 434032 boundary elements. These elements have an average quality of 0.581. For the narrow channels, in order to capture the thermal-fluid effects better, 8 elements are distributed in the radial direction. The first wide channel, in which thermal-fluid effects are also important, is divided in 20 elements in the radial direction with a heterogeneous distribution (more elements near to heat exchange surface).

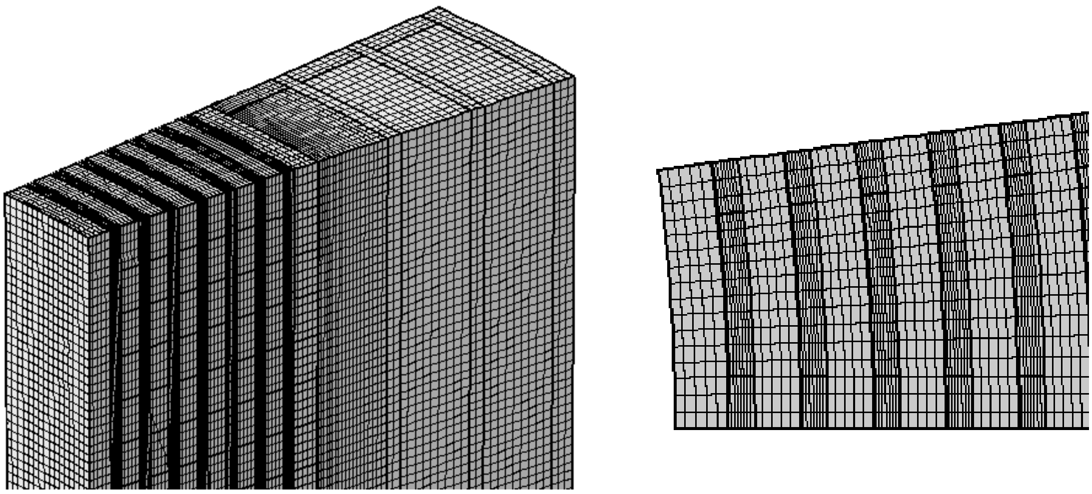

Fig. 4. Meshing of the model

Regarding the computational information, the simulations took between 170 and 230 minutes using a physical RAM of 30.4 GB of a workstation Dell Precision T5500, with two Intel Xeon X5650 processors (6 cores/processor), 2.66GHz and 48 GB RAM. An error lower than 10^{-4} was used as a convergence criterion in the simulations.

2.2.4. Material properties

The Fig. 5 presents the four physical properties of the liquids that are used in the numerical model by means of graphical plots in the range of operating temperatures. The data were provided by the manufacturers of the oils. The densities of all the liquids decrease with temperature linearly with very similar slope. In the case of the viscosities, at low temperatures, natural esters have higher values than that of the mineral oil. However, this property diminishes exponentially with the temperature, this being alike at high temperatures for the three liquids. Regarding thermal conductivities, these decrease slowly with temperature in all the cases. Finally, the specific heat capacities of the three liquids increases with temperature.

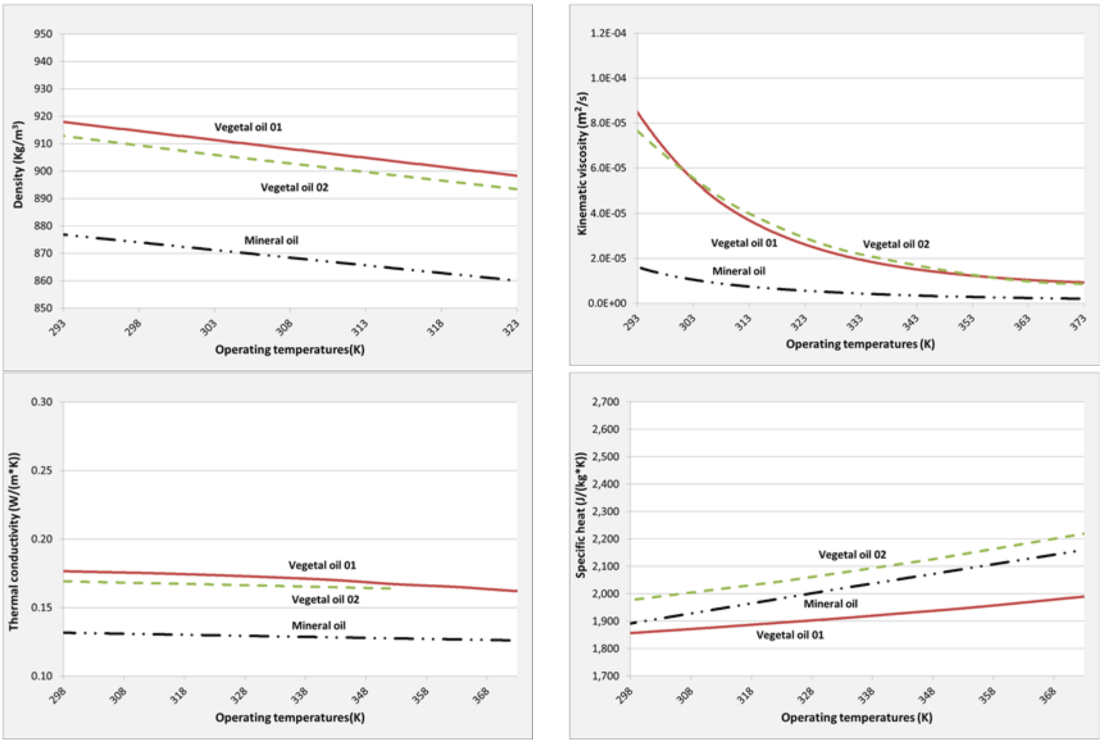

Fig. 5. Physical properties of the dielectric liquids

The winding layers are made of copper conductors that are individually wrapped with dielectric paper. Also, these layers and four cardboard cylinders are separated by wooden sticks and inter-sticks. The physical properties (density, ρ; thermal conductivity, k; and ,thermal capacity, C_p) that are needed for all these materials in order to use them in the simulations are shown in Table 1. These properties are assumed to be constant with temperature.

Table 1. Physical properties of solid materials.

	ρ [kg/m³]	k [W/(m K)]	C_p [J/(kg K)]
Copper	8,700	400	385
Paper	930	0.19	1,340
Cardboard	1,150	0.25	2,093.5
Wood	418.5	0.15	2,720

2.3. Model validation and results comparison

In this point, dimensionless parameters are determined in order to reaffirm the validity of the model. Later, simulation results are presented.

2.3.1. Model validation

In order to confirm the boundary assumptions: natural convection in laminar regime, two dimensionless parameters are calculated, Reynolds (Re) and Grashoff (Gr) numbers (See Eqs. (12) and (13), in which β is the thermal expansion coefficient and L is characteristic length (hydraulic diameter). Also, the physical properties are obtained at *Toil,outlet* and u is the average velocity in the outlet).

$$Re = \frac{Inertial\ forces}{Viscous\ forces} = \frac{\rho \cdot u \cdot L}{\mu} \quad (12)$$

$$Gr = \frac{Buoyancy\ forces}{Viscous\ forces} = \frac{g \cdot \beta \cdot \Delta T \cdot L^3 \cdot \rho^2}{\mu^2} = \frac{g \cdot \frac{\rho(273{,}15) - \rho(T_{oil,outlet})}{\rho(T_{oil,outlet}) \cdot (T_{oil,outlet} - 273.15)} \cdot (T_{oil,outlet} - T_{oil,inlet}) \cdot L^3 \cdot \rho^2}{\mu^2} \quad (13)$$

The Reynolds number represents the ratio between the inertial and viscous forces. In other words, this parameter can be used to determine if the coolant flow through the channels is laminar (Re < 2100) or turbulent (Re > 4000). Regarding the type of convection, the ratio Gr/Re^2 can be used to determine whether it is forced convection ($Gr/Re^2 << 1$) or natural convection ($Gr/Re^2 >> 1$) [29]. As can be seen in Table 2, all the studied liquids are clearly in laminar regime in all the ducts. Regarding the type of convection, the values of Gr/Re^2 reaffirm the assumption of natural convection.

Table 2. Dimensionless numbers

		Channels									
		1	2	3	4	5	6	7	8	9	10
Mineral oil	Re	9.36	13.94	14.61	14.61	14.52	14.45	14.23	30.20	1.22	0.48
	Gr/Re^2	12.62	8.17	8.09	8.21	8.26	8.20	7.32	3.24	80.83	204.51
Vegetal oil 01	Re	1.94	2.68	2.85	2.87	2.85	2.73	2.34	4.05	0.18	0.08
	Gr/Re^2	81.94	56.02	53.75	54.03	53.76	53.09	51.69	18.52	551.39	1273.23
Vegetal oil 02	Re	1.75	2.53	2.74	2.76	2.72	2.56	2.06	3.54	0.16	0.07
	Gr/Re^2	96.21	65.30	62.57	62.91	62.67	62.04	60.98	21.33	613.97	1420.29

2.3.2. Results

The Table 3 shows the maximum temperature of the geometry, $T_{max\ model}$, the outlet average temperature, $T_{avg\ outlet}$, and the mass flow rate, in all the ducts for all the liquids.

Table 3. Temperatures in the geometry and mass flow rates in cooling ducts.

		Channels										$T_{max\ model}$ (°C)
		1	2	3	4	5	6	7	8	9	10	
Mineral oil	$T_{avg\ outlet}$ (°C)	60.5	64.1	64.7	64.6	64.8	62.9	57.9	36.7	35.1	35.0	69.0
	$\dot{m}_{ch}$ (g/s)	0.36	0.53	0.58	0.61	0.67	0.66	0.60	5.83	0.23	0.10	
Vegetal oil 01	$T_{avg\ outlet}$ (°C)	83.2	87.1	88.1	87.9	87.3	83.0	73.1	38.8	35.3	35.1	91.3 (ΔT= 22.3)
	$\dot{m}_{ch}$ (g/s)	0.21	0.32	0.35	0.37	0.40	0.39	0.34	3.71	0.19	0.09	
Vegetal oil 02	$T_{avg\ outlet}$ (°C)	83.7	87.6	88.6	88.4	87.8	83.5	73.6	38.9	35.3	35.1	91.8 (ΔT= 22.8)
	$\dot{m}_{ch}$ (g/s)	0.19	0.27	0.30	0.32	0.35	0.33	0.29	3.25	0.17	0.08	

In all the cases, the highest oil temperatures, $T_{avg\ outlet}$, appear in inner ducts, Table 3. In the case of vegetal oils, these temperatures are about 23ºC higher than those of mineral oil.

In relation to the $T_{max\ model}$, it can be seen that if the ester-based liquids are used instead of the mineral oil there is an increase of about 22ºC. Also, the location of these hot-spots for the three dielectric liquids are situated in the same position; that is, they are located on the top of the geometry, in middle of the third layer of the winding, at the symmetry plane (See Fig. 6). This coincidence is justified in the fact that the location of the hot-spots only depend on the numerical model developed, on the boundary conditions established and on the type of geometry considered; it does not depend on the type of liquid.

Regarding m_{ch} and velocities, it can be observed that the ester-based liquids have lower values due to, mainly, their high viscosities. In this case, the oil cooling capacities are more influenced by changes in oil flow than by the specific heat of the fluid used. So, the cooling capacities of these two ester liquids are worse than those of the mineral: there are higher temperatures in the winding with esters.

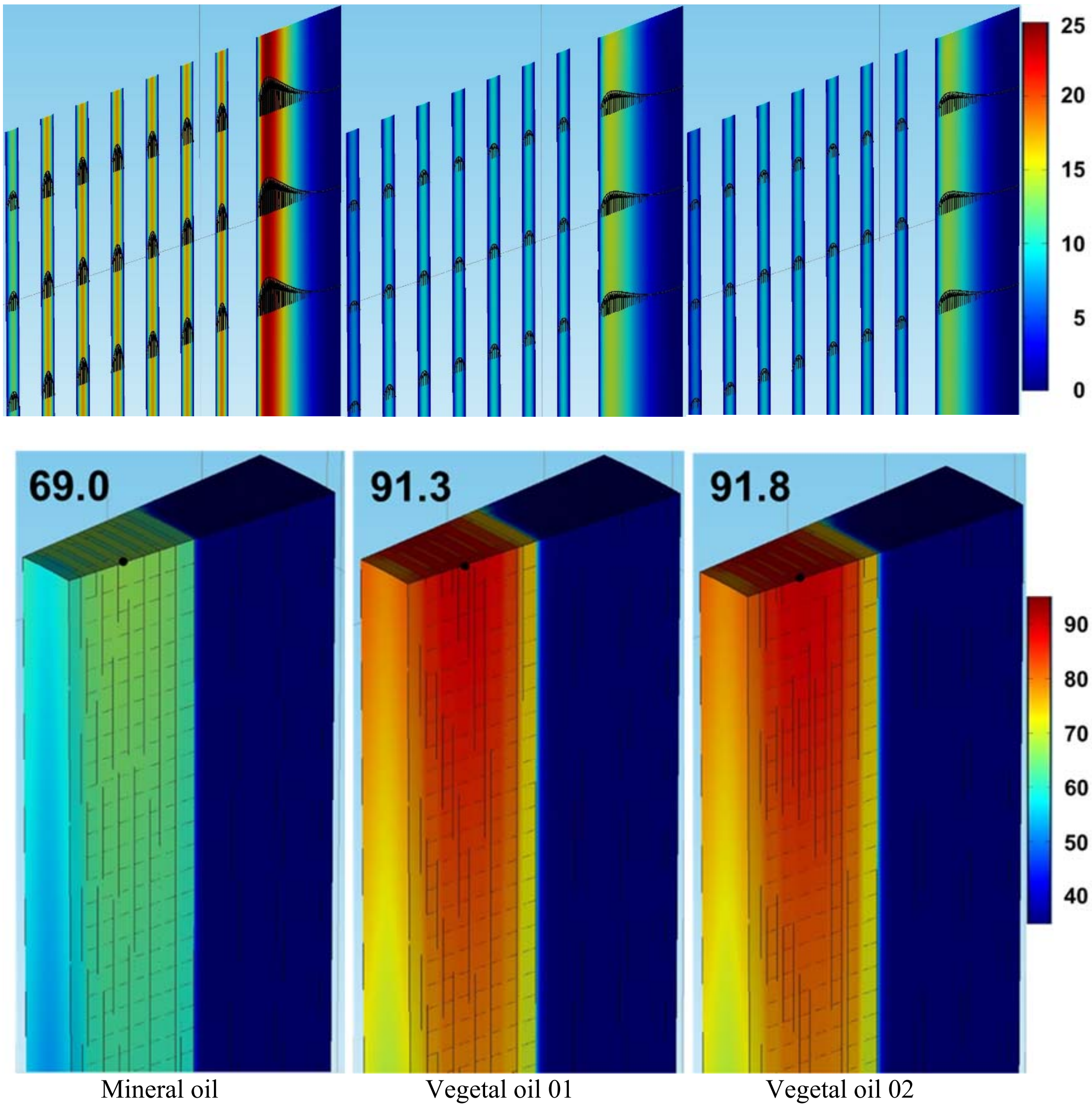

Fig. 6. Temperature (ºC) and velocities (mm/s) distributions of studied liquids

3. Thermal-ageing of Kraft paper

The evolution of aging in the insulation system of power transformers is mainly connected with the temperature profile. Thus, once the differences between the temperatures reached in the hot spot by mineral and vegetable oils has been obtained in the previous section for a transformer winding, approximately 20ºC, the following step is to evaluate the Kraft paper degradation in mineral and vegetable oils at different temperatures. It is well known that aging experiments made in laboratory under operating conditions of power transformers require huge periods of time and high costs. For these reasons, controlled laboratory scale experiments have to introduce conditions for rapid deterioration on insulation to quantify its failure. Currently, the standardized method used to evaluate the solid insulation lifetime in power transformers is based on the IEC 60216-1/2001 [30] which establishes that the insulation material shall be submitted to aging at three different temperatures.

3.1. Materials and methods

A thermal aging study of Kraft paper in different types of dielectric oils (two natural esters oils and a mineral oil) was implemented in the laboratory. The three aging temperatures were 110, 130 and 150ºC, keeping 20°C difference between each test. This temperature range is higher than the operating temperatures in a power transformer, but gives significant degradation in a reasonable time scale. The condition of insulating paper was studied through DP measurements which were performed on samples taken out at different aging periods. For each aging temperature chosen, the aging time was extended to the time required to reach the end of life criterion for Kraft paper in mineral oil. When DP value falls below 200 it is considered that the insulating paper has reached the end of its life [8].

In order to monitor the ageing of Kraft paper in dielectric oils over time at different temperatures, the samples were prepared in several steps. Firstly, Kraft paper was cut into 260 mm long and 15 mm wide strips, Fig. 7, and dried under vacuum at 100ºC for one day. Secondly, three steel vessels (1 liter each) were filled with 800 ml oil and 60 strips of Kraft paper, Fig. 7. Some characteristics about the Kraft paper used in thermal aging are given in Table 4. These data have been provided by manufacturers.

Fig. 7. Kraft paper strips and steel vessel.

Table 4. *Properties of analysed Kraft paper.*

Property	Units	Standard	Value
Thickness	mm	IEC 60554-2	0.2
Grammage	g / m^2		149.3
Apparent density	kg / m^3		754
Electric strength in air	kV / mm		8.9

Once oil and Kraft paper had been introduced in steel vessels; vacuum and nitrogen filling were carried out to have the head space above the oil filled with nitrogen. Subsequently, the steel vessels were placed inside an oven adjusted to 110, 130 and 150ºC. At intervals increasing with ageing time, samples of Kraft paper were taken. The Kraft paper aging was monitored over time through the DP of the specimens. These values of DP were obtained according to ASTM D4243 [31]. Each paper was first de-oiled using fresh hexane. Later paper samples were dissolved in copper ethylenediamine (CUEN) solvent, and its viscosity measured using an automatic viscometer equipped with a two-sphere Ubbelohde tube, Fig. 8.a. The paper moisture was determined by titration using a Karl-Fischer coulometer, Fig.8.b. Solution viscosity and paper moisture are the parameters used to estimate the DP.

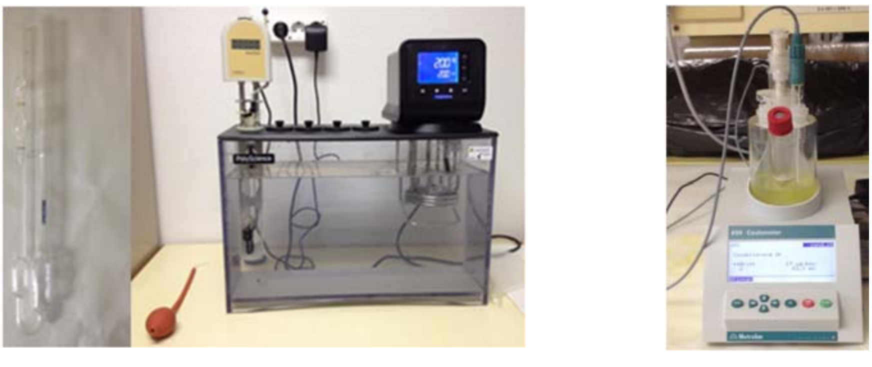

a) Automatic viscometer b) Karl-Fischer coulometer

Fig. 8. Laboratory equipment

3.2. Results

The results indicate that the rate of paper aging is fluid-dependent. Considering the same temperature, paper aged in mineral oil degraded at a significantly faster rate than in vegetable dielectric fluids (see Figs. 9-11). At the three temperatures, the degradation rate of Kraft paper immersed in "vegetable oil 01" was a little higher than that immersed in "vegetable oil 02" at the early aging stage. However, it decreased gradually with the development of the aging process and is finally slower than in "vegetable oil 02". If 200 DP is considered as the endpoint of life, the lifetimes of Kraft paper in mineral oil at 110, 130 and 150ºC are about 2100, 1080 and 50 hours respectively. The other samples, Kraft paper aging at the same temperatures in natural esters, do not reach their endpoint of life by the end of aging tests. Therefore, vegetable oils retard the degradation rate of Kraft paper and extend its useful lifetime.

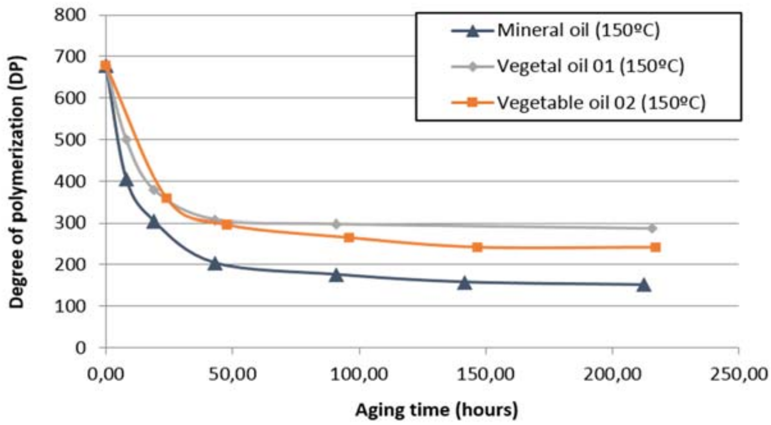

Fig. 9. Evolution of DP with the aging period (150ºC).

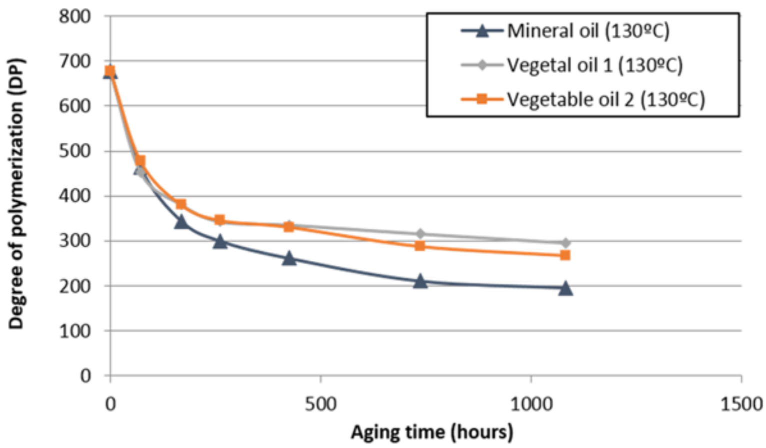

Fig. 10. Evolution of DP with the aging period (130ºC).

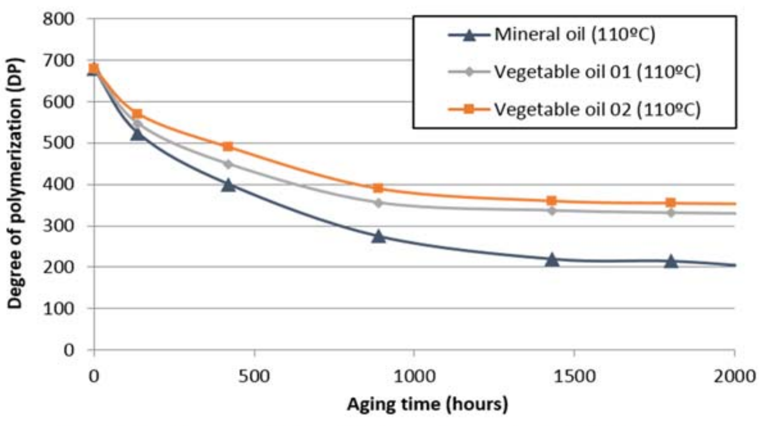

Fig. 11. Evolution of DP with the aging period (110ºC).

Nevertheless, it is necessary to consider that the cooling capacity of vegetable oils is lower than that of the mineral oil, as it was obtained through the simulations in previous section. In this work, it was obtained that for a section of the LVW of a three-phase power transformer the hot-spot temperature in the case of vegetables oils increases around 20ºC in comparison with mineral oil. If this difference of temperature is considered when degradation rate of Kraft paper in mineral and vegetable oils is compared, the results change. For instance, Fig. 12 compares the evolution of the DP value of Kraft paper in mineral oil at 130ºC with the evolution in vegetable oils at 150ºC. It can be observed that degradation rate of Kraft paper at the end of aging period tend to a similar value in the three oils. The substitution of a mineral oil by a vegetal ester causes that the paper suffers higher temperature in the transformer winding, but in a less aggressive environment for cellulose. The tests have shown that these effects are practically compensated each other.

The Fig. 13 shows the evolution of the DP value of Kraft paper in mineral oil at 110ºC and the evolution in natural esters at 130ºC. At the early aging stage, the degradation rates of Kraft paper immersed in natural esters were higher than that immersed in mineral oil. Nevertheless, they diminished with the aging process and they are finally quite similar to the mineral oil. As in the previous case, it can be observed that the higher hot-spot temperature obtained with vegetables oils reduces their positive effect on the degradation rate of Kraft paper.

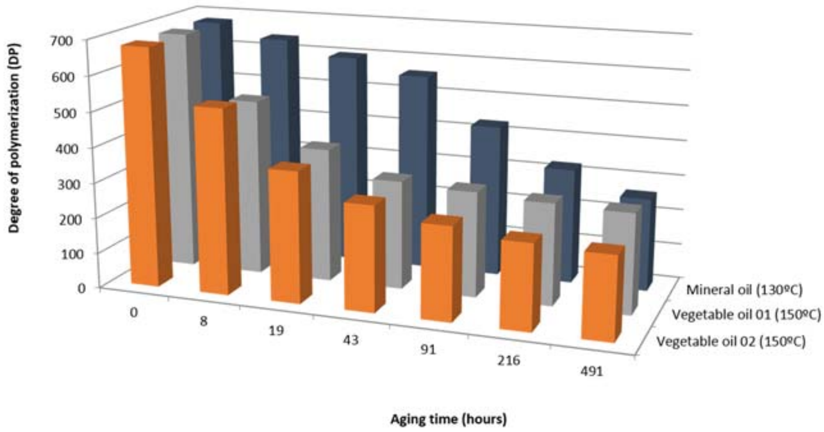

Fig. 12. Evolution of DP with the aging period (Mineral 130ºC-Vegetal 150ºC).

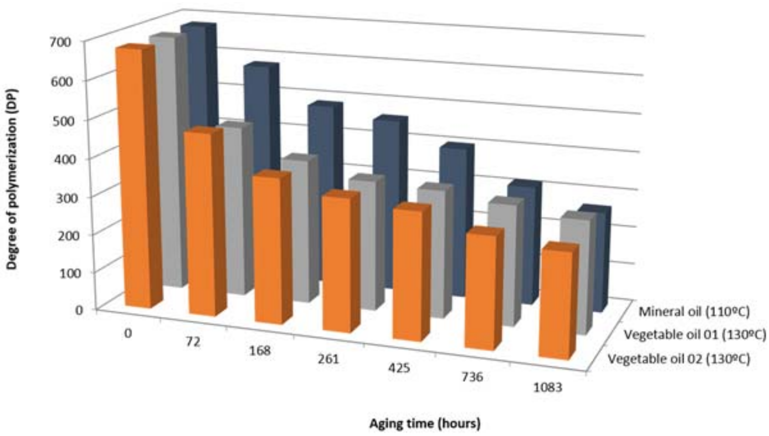

Fig. 13. Evolution of DP with the aging period (Mineral 110ºC-Vegetal 130ºC).

4. Conclusions

Dielectric oils based on natural esters might be suitable substitutes for mineral oil due to their higher biodegradability, fire safety and availability. However, when a new material is to be introduced to a system as a power transformer, the rate of degradation of the new insulation system has to be evaluated. In order to assess the performance of new insulating systems based on natural esters oils, simulations about cooling in power transformers using vegetable oils and controlled laboratory experiments have been carried out.

In this article, a simulation of a section of the low voltage winding of a three-phase power transformer has been carried out in order to obtain the hot-spot temperatures. This has been performed for two vegetable oils and one mineral oil. The simulation results were used to define the thermal aging conditions applied to degradation experiments of Kraft paper.

In this transformer, the difference of hot-spot temperatures obtained with mineral oil is around 20ºC lower than the ones obtained with vegetable oils. This is due to the fact that natural esters possess a lower cooling capacity. This difference in hot spot temperatures increases considerably the thermal stress suffered by Kraft paper inside power transformers when vegetal oil is used.

The aging experiments carried out at the same temperature, show that the dielectric paper is less degraded by the vegetable oils, which extends considerably useful lifetime of Kraft paper. However, taking into account that this type of oils show a higher hot-spot temperature, the aging test temperature must be increased by 20ºC with respect to the mineral oil aging tests (110- 130ºC and 130-150 ºC). The results of this last comparison shows that the degradation rate of Kraft paper is quite similar at the end of aging period.

Therefore, for a specific geometry of power transformer, it has been shown that isolation paper suffers worse thermal conditions when it is immersed in vegetable oils; however the physical properties of these oils also extend the lifespan of this paper. Both effects tend to the balance in the long term and the degradation is similar to the one obtained in windings cooled by mineral oil. This way, owners of similar transformers, could substitute mineral oil by biodegradable oil, without any significant increase in speed of dielectric paper degradation. In other transformers, a similar study should be implemented in order to analyze the viability of the change of mineral oil by a natural ester.

ACKNOWLEDGMENTS

The research leading to these results has received funding from multiple sources during years but we would specifically like to acknowledge the support received in the later stages from the Spanish Plan Estatal de I+D under the grant agreement DPI2013-43897-P.

REFERENCES

[1] M.S. Godinho, M.R. Blanco, F.F. Gambarra, L.M. Lião, M.M. Sena, R. Tauler, A.E. de Oliveira, Evaluation of transformer insulating oil quality using NIR, fluorescence, and NMR spectroscopic data fusion, Talanta 129 (2014) 143-149. DOI:10.1016/j.talanta.2014.05.021
[2] E.I. Koufakis, C.G. Karagiannopoulos, P.D. Bourkas, Thermal coefficient measurements of the insulation in distribution transformers of a 20 kv network, Measurement 41 (2008) 10-19. DOI:10.1016/j.measurement.2007.02.002
[3] W.C. Flores, E.E. Mombello, J.A. Jardini, G. Rattá, A.M. Corvo, Expert system for the assessment of power transformer insulation condition based on type-2 fuzzy logic systems, Exp. Syst. Appl. 38 (2011) 8119-8127. DOI:10.1016/j.eswa.2010.12.153
[4] L. Yang, R. Liao, S. Caixin, M. Zhu, Influence of vegetable oil on the thermal aging of transformer paper and its mechanism, IEEE Trans. Dielectr. Electr. Insulation 18 (2011) 692-700. DOI: 10.1109/TDEI.2011.5931054
[5] L.M. Dumitran, R. Setnescu, P.V. Notingher, L.V. Badicu, T. Setnescu, Method for lifetime estimation of power transformer mineral oil, Fuel 117 (2014) 756-762. DOI:10.1016/j.fuel.2013.10.002
[6] M.L. Coulibaly, C. Perrier, M. Marugan, A. Beroual, Aging behavior of cellulosic materials in presence of mineral oil and ester liquids under various conditions, IEEE Trans. Dielectr. Electr. Insulation 20 (2013) 1971-1976. DOI: 10.1109/TDEI.2013.6678843
[7] H. El-Saied, M.G. El-Meligy, S.H. Mohamed, S.A. El-Mongy, Electrical insulated paper from cotton linter, Carbohyd. Polym. 90 (2012) 147-151. DOI: 10.1016/j.carbpol.2012.05.007
[8] A. Susilo, Suwarno, U. Khayam, M. Tsuchie, M. Thein, M. Hikita, T. Saito, Study on dissolved gas due tue thermally degraded insulating paper in transformer oil. Procedia Technol. 11 (2013) 257-262. DOI:10.1016/j.protcy.2013.12.189
[9] M.H.G. Ese, K.B. Liland, C. Lesaint, M. Kes, Esterification of low molecular weight acids in cellulose, IEEE Trans. Dielectr. Electr. Insulation 21 (2014) 662-665. DOI: 10.1109/TDEI.2013.004238
[10] E.O. dos Santos, A.M. Santana Silva, W.D. Fragoso, C. Pasquini, M.F. Pimentel, Determination of degree of polymerization of insulating paper using near infrared spectroscopy and multivariate calibration, Vib. Spectrosc. 52 (2010) 154-157. DOI: 10.1016/j.vibspec.2009.12.004

[11] R. Setnescu, L.V. Badicu, L.M. Dumitran, P.V. Notingher, T. Setnescu, Thermal lifetime of cellulose insulation material evaluated by an activation energy based method, Cellulose 21 (2014) 823-833. DOI: 10.1007/s10570-013-0087-0
[12] N. Lelekakis, J. Wijaya, D. Martin, T. Saha, D. Susa, C. Krause, Aging rate of grade 3 presspaper insulation used in power transformers, IEEE Trans. Dielectr. Electr. Insulation 21 (2014) 2355-2362. DOI: 10.1109/TDEI.2014.004266
[13] T. Łojewski, P. Miśkowiec, M. Missori, A. Lubańska, L.M. Proniewicz, J. Łojewska, FTIR and UV/vis as methods for evaluation of oxidative degradation of model paper: DFT approach for carbonyl vibrations, Carbohydr. Polym. 82 (2010) 370-375. DOI: 10.1016/j.carbpol.2010.04.087
[14] T. Łojewski, K. Zieba, A. Kołodziej, J. Łojewska, Following cellulose depolymerization in paper: comparison of size exclusion chromatography techniques, Cellulose 18 (2011) 1349-1363. DOI:10.1007/s10570-011-9562-7
[15] H. Malik, A.K. Yadav, S. Mishra, T. Mehto, Application of neuro-fuzzy scheme to investigate the winding insulation paper deterioration in oil-immersed power transformer, Int. J. Electr. Power Energy Syst. 53 (2013) 256-271. DOI: 10.1016/j.ijepes.2013.04.023
[16] P.E. Sánchez-Jiménez, L.A. Pérez-Maqueda, A. Perejón, J. Pascual-Cosp, M. Benítez-Guerrero, J.M. Criado, An improved model for the kinetic description of the thermal degradation of cellulose, Cellulose 18 (2011) 1487-1498. DOI:10.1007/s10570-011-9602-3
[17] A. Baral, S. Chakravorti, Condition assessment of cellulosic part in power transformer insulation using transfer function zero of modified debye model, IEEE Trans. Dielectr. Electr. Insulation 21 (2014) 2028-2036. DOI: 10.1109/TDEI.2014.004517
[18] H.C. Sun, Y.C. Huang, C.M. Huang, A Review of dissolved gas analysis in power transformers, Energy Procedia 14 (2012) 1220-1225. DOI: 10.1016/j.egypro.2011.12.1079
[19] I. Fernández, A. Ortiz, F. Delgado, C. Renedo, S. Pérez, Comparative evaluation of alternative fluids for power transformers, Electr. Power Syst. Res. 98 (2013) 58-69. DOI: 10.1016/j.epsr.2013.01.007
[20] M.K. Pradhan, Assessment of the status of insulation during thermal stress accelerated experiments on transformer prototypes. IEEE Trans. Dielectr. Electr. Insulation 13 (2006) 227-237. DOI: 10.1109/TDEI.2006.1593420
[21] J. Coddé, W. Van der Veken, M. Baelmans, Assessment of a hydraulic network model for zig-zag cooled power transformer windings, Appl. Therm. Eng. 80 (2015) 220-228. DOI: 10.1016/j.applthermaleng.2015.01.063
[22] R. Sitar, Z. Janié, Z. Stih, Improvement of thermal performance of generator step-up transformers, Appl Therm. Eng. 78 (2015) 516-524. DOI: 10.1016/j.applthermaleng.2014.12.052
[23] F. Torriano, P. Picher, M. Chaaban, Numerical investigation of 3D flow and thermal effects in a disc-type transformer winding, Appl. Therm. Eng. 40 (2012) 121-131. DOI: 10.1016/j.applthermaleng.2012.02.011
[24] F. Delgado, A. Ortiz, I. Fernández, A. Arroyo, J.A. Macias, Study on the cooling capacity of alternative liquids in power transformers, Conf. Electr. Systems Aircr., Railway and Ship Propulsion - ESARS (2012) 1-6. DOI: 10.1109/ESARS.2012.6387482
[25] S. Han, Q. Li, C. Li, J. Yan, Electrical and mechanical properties of the oil-paper insulation under stress of the hot spot temperature, IEEE Trans. Dielectr. Electr. Insulation 21 (2014) 179-185. DOI: 10.1109/TDEI.2013.003967
[26] V.A. Yatsevsky, Hydrodynamics and heat transfer in cooling channels of oil-filled power transformers with multicoil windings, Appl. Therm. Eng. 63 (2014) 347-353. DOI: 10.1016/j.applthermaleng.2013.10.055
[27] A. Skillen, A. Revell, H. Iacovides, W. Wu, Numerical prediction of local hot-spot phenomena in transformer windings, Appl. Therm. Eng. 36 (2012) 96-105. DOI: 10.1016/j.applthermaleng.2011.11.054
[28] M.A.G. Martins, Vegetable oils, an alternative to mineral oil for power transformers – experimental study of paper aging in vegetable oil versus mineral oil, IEEE Elect. Insul. Mag. 26 (2010) 7– 13. DOI: 10.1109/TDEI.2013.6678843
[29] F. Torriano, M. Chaaban, and P. Picher, Numerical study of parameters affecting the temperature distribution in a disc-type transformer winding, Appl. Therm. Eng. 30 (2010) 2034– 2044. DOI:10.1016/j.applthermaleng.2010.05.004
[30] IEC 60216-1:2013 Electrical insulating materials – Thermal endurance properties – Part 1: Ageing procedures and evaluation of test results.
[31] ASTM D4243-99(2009) Standard test method for measurement of average viscometric degree of polymerization of new and aged electrical papers and boards.